Dalton Transactions

RSC Publishing

PAPER

View Article Online
View Journal | View Issue

Fixed-charge phosphine ligands to explore gas-phase coinage metal-mediated decarboxylation reactions†

Cite this: *Dalton Trans.*, 2013, **42**, 6440

Krista Vikse,[a,b] George N. Khairallah,[a,b] J. Scott McIndoe[c] and Richard A. J. O'Hair*[a,b]

A combination of multistage mass spectrometry experiments and density functional theory (DFT) calculations were used to examine the decarboxylation reactions of a series of metal carboxylate complexes bearing a fixed-charge phosphine ligand, $[(O_3SC_6H_4)(C_6H_5)_2PM^{I}O_2CR]^-$ (M = Cu, Ag, Au; R = Me, Et, benzyl, Ph). Collision-induced dissociation (CID) of these complexes using an LTQ linear ion mass spectrometer results in three main classes of reactions being observed: (1) decarboxylation; (2) loss of the phosphine ligand; (3) loss of carboxylic acid. The gas-phase unimolecular chemistry of the resultant decarboxylated organometallic ions, $[(O_3SC_6H_4)(C_6H_5)_2PM^{I}R]^-$, were also explored using CID experiments, and fragment primarily *via* loss of the phosphine ligand. Energy-resolved CID experiments on $[(O_3SC_6H_4)(C_6H_5)_2PM^{I}O_2CR]^-$ (M = Cu, Ag, Au; R = Me, Et, benzyl, Ph) using a Q-TOF mass spectrometer were performed to gain a more detailed understanding of the factors influencing coinage metal-catalyzed decarboxylation and DFT calculations on the major fragmentation pathways aided in interpretation of the experimental results. Key findings are that: (1) the energy required for loss of the phosphine ligand follows the order Ag < Cu < Au; (2) the ease of decarboxylation of the coordinated RCO_2 groups follows the order of R: Ph < $PhCH_2$ < Me < Et; (3) in general, copper is best at facilitating decarboxylation, followed by gold then silver. The one exception to this trend is when R = Ph and M = Au which has the highest overall propensity for decarboxylation. The influence of the phosphine ligand on decarboxylation is also considered in comparison with previous studies on metal carboxylates that do not contain a phosphine ligand.

Received 28th September 2012,
Accepted 20th February 2013

DOI: 10.1039/c3dt32285h

www.rsc.org/dalton

Introduction

Interest in the decarboxylation of metal carboxylates is currently high due to the relevance of this reaction to catalytic transformations in organic synthesis. Specifically, a metal catalyst capable of efficiently transforming inexpensive carboxylate salts into decarboxylated carbon-based nucleophiles bypasses the need for expensive organometallic reagents currently required in stoichiometric amounts for many C–C bond-forming reactions. In the search for the ideal catalyst, a wide range of metals and ligands have been surveyed. The synthetic utility of the same organometallic complexes in C–C bond-forming reactions has also been explored. Recent reviews highlight progress on both fronts.[1–6]

Coinage metal complexes show considerable promise at promoting decarboxylation. Indeed, copper-mediated decarboxylation reactions date back to the seminal work of Shepard *et al.* in 1930 on the copper/quinoline-catalyzed thermal decarboxylation of aromatic carboxylic acids.[7] Subsequent mechanistic work in the 1960s and 1970s by the groups of Nilsson,[8–10] Cohen[11,12] and Cairncross[13] established that organocopper species are formed as intermediates. More recently, Goossen has developed a protocol for catalytic protodecarboxylation of a large range of aromatic carboxylic acids, including deactivated substrates, using copper phenanthroline catalysts.[14,15] Shang *et al.* employed a similar catalyst to promote the decarboxylative cross-coupling of polyfluorobenzoates with arylhalides to yield polyfluorobiaryls, which are useful molecules in both medicinal chemistry and materials science.[16] In this work, copper successfully facilitates both decarboxylation and the subsequent cross-coupling reaction. Silver salts have also recently gained attention as effective protodecarboxylation catalysts. Under optimized conditions they can promote reactions at much lower temperatures than typical copper catalysts, and transform *ortho*-substituted or heterocyclic derivatives that failed to react with copper catalysts.[17–19] Finally, the ability of gold(I) complexes to

[a]*School of Chemistry, The University of Melbourne, Victoria 3010, Australia. E-mail: rohair@unimelb.edu.au; Tel: +61 3 8344-2452; Fax: +61 3 9347-5180*
[b]*Bio21 Institute of Molecular Science and Biotechnology, The University of Melbourne, Victoria 3010, Australia*
[c]*Department of Chemistry, University of Victoria, P. O. Box 3065, Victoria, BC V8W 3V6, Canada*

† Electronic supplementary information (ESI) available: Complete citation for ref. 43 Cartesian coordinates and energies for all DFT calculated species, and additional mass spectra. See DOI: 10.1039/c3dt32285h

stoichiometrically decarboxylate aromatic carboxylic acids has been very recently reported. A higher degree of selectivity for decarboxylation (over protodemetallation) and lower possible reaction temperatures were noted for the gold complexes as compared to copper- and silver-based systems and work in this area is now focused on developing catalytic reactions using gold(I).[20,21]

Metal-mediated decarboxylation reactions can also be studied in the gas phase where detailed mechanistic information can be gained for reactive intermediates that are difficult or impossible to isolate in solution. Such studies utilise mass spectrometric methods,[22,23] in which complexes of the coinage metal carboxylates must carry either a positive or negative charge. This can be achieved *via* the use of: (1) a second carboxylato ligand, $R'CO_2$, to form a complex of the type $[R'CO_2M^IO_2CR]^-$, which allows dialkyl metallates, $[R'M^IR]^-$, to be "synthesized" *via* sequential, double decarboxylation reactions;[24–35] (2) a second metal cation, M′, to form a complex of the type $[RCO_2M^IM^{I\prime}]^+$, which forms the binuclear bridged organometallic complexes $[RM^IM^{I\prime}]^+$;[36,37] and (3) a fixed-charge auxillary ligand, L, to bind to the metal center and thus acts as a "charge handle".[38,39] The fixed-charge auxillary ligand can either hold a positive charge to yield a complex, $[LM^IO_2CR]^+$, that can be examined in the positive ionization mode, or can hold a negative charge to yield a complex, $[LM^IO_2CR]^-$, that can be examined in the negative ionization mode. This method of installing a charge has the key advantage that the charge site is remote from the site of reaction. Therefore, the charge-tagged complex is much more likely to exhibit the same reactivity and characteristics as its neutral analogue. While fixed-charge auxillary ligands have been used to facilitate the observation of organometallic species *via* electrospray ionization mass spectrometry (ESI/MS),[38,39] here we demonstrate that they can be used to examine the gas-phase decarboxylation reactions of coinage metal complexes bearing the fixed-charge phosphine ligand $(C_6H_5)_2P(C_6H_4SO_3)^-$ (triphenylphosphine monosulfonate or TPPMS, Scheme 1).

Here we aim to use M^I(TPPMS) complexes (M = Cu, Ag, Au) of acetate (**1a-c**), propionate (**2a-c**), phenylacetate (**3a-c**), and benzoate (**4a-c**) to examine how addition of a phosphine ligand influences coinage metal-catalyzed decarboxylation reactions. We will compare our findings to solution-phase work and related gas-phase systems.[26,27,30] To that end, energy-resolved CID[40–42] and multistage mass spectrometry experiments were performed on $[(TPPMS)M^IO_2CR]^-$ complexes (**1(a-c)–4(a-c)**) to determine their unimolecular reactivity.

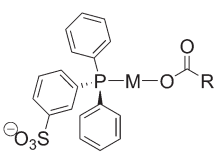

1(a-c): R = Me M = Cu^I, Ag^I, Au^I
2(a-c): R = Et M = Cu^I, Ag^I, Au^I
3(a-c): R = CH_2Ph M = Cu^I, Ag^I, Au^I
4(a-c): R = Ph M = Cu^I, Ag^I, Au^I

Scheme 1 Coinage metal carboxylate complexes bearing the fixed-charge phosphine ligand TPPMS, $(C_6H_5)_2P(C_6H_4SO_3)^-$.

Density functional theory (DFT) calculations are included and aid in the interpretation of experimental data.

Experimental section

Reagents

Methanol, copper(II)acetate, silver(I)acetate, gold(III)acetate, acetic acid, propionic acid, benzoic acid, and phenylacetic acid were obtained from Aldrich and used without further purification. Bis(triphenylphosphine)iminium triphenylphosphine monosulfonate was synthesized as reported previously.[38c,43]

Mass spectrometry

Methanol solutions of 0.1 mM $[(PPh_3)_2N][P(C_6H_5)_2(C_6H_4SO_3)]$ (*i.e.* [PPN][TPPMS]), 0.5 mM $M(O_2C_2H_3)_n$ (M = Cu^{II}, Ag^I, Au^{III} and n = 2, 1, 3, respectively) and, where required, 2 mM HO_2CR (R = C_2H_5, C_6H_5,$CH_2C_6H_5$) were prepared under N_2. The solutions were allowed to stir for approximately 1 min before analysis using a Micromass Q-TOF *micro* hybrid quadrupole/time-of-flight mass spectrometer or a modified Thermo Finnigan LTQ linear ion trap mass spectrometer coupled with an FT-ICR cell:[44] both equipped with electrospray ionization.

LTQ – Solutions were pumped *via* syringe into the electrospray source at a rate of 5 μL min^{-1}. Typical electrospray source conditions were: needle potential: 4.0–5.0 kV, heated capillary temperature: 250–300 °C. The desired precursor ion was mass selected and subjected to CID in the LTQ using standard isolation and excitation procedures. High-resolution mass spectrometry data were obtained by transferring ions of interest from the linear ion trap into the FT-ICR cell. Good accurate mass and isotope pattern matches (data not shown) provide unambiguous assignment of all complexes **1(a-c)–4(a-c)**.

Q-TOF – Solutions were pumped *via* syringe into the electrospray source at a rate of 10 μL min^{-1}. Instrument conditions were set as follows: capillary voltage: 2900 V, cone voltage: 20 V, extraction voltage: 0.5 V, source temperature: 80 °C, desolvation temperature: 150 °C, cone gas: 100 L h^{-1}, desolvation gas: 100 L h^{-1}, ion energy: 2.0 V, low/high mass resolution: 14.0, collision energy: 2 V for standard MS and 0–40 V for energy-dependent CID, collision cell pressure: 2.77 ± 0.01 × 10^{-5} torr, MCP: 2700 V.

DFT calculations

Gaussian 09[45] utilizing the B3LYP hybrid functional[46,47] was employed for all geometry optimizations and vibrational frequency calculations. The Stuttgart Dresden (SDD) basis set and effective core potential were used for the metal atoms while the 6-31+G(d) all electron basis set was used for carbon, oxygen and hydrogen.[48–52] This combination was chosen due to constraints imposed by the sizes of the metal complexes studied (32 heavy atoms for the largest complex) and to allow direct comparison with our previous work.[26,27,30] Condensed-phase calculations were carried out using a solvent continuum. All transition state geometries were characterized by the

presence of a single imaginary frequency. Due to the sizes of the metal complexes studied, intrinsic reaction coordinates (IRC) were carried out only on the acetate complexes, $[(TPPMS)M^{I}O_2CCH_3]^-$, using default parameters to ensure smooth connection of reactants and products. In the forward direction of these IRC calculations, weakly bound ion-neutral complexes between the organometallic, $[(TPPMS)M^{I}CH_3]^-$, and the departing CO_2 appear to be forming, although these we not fully optimized due to the large number of steps required to optimize these types of complexes. All quoted energies include zero point vibrational energy.

Results and discussion

1. Choice of phosphine ligand and binding mode to coinage metals

The negatively charged phosphine analogue, TPPMS, provides a well-behaved electrospray-active analogue for the otherwise neutral metal complexes $PPh_3M^{I}O_2CR$. The charged group is in the *meta* position on one of the phenyl groups of the ligand and this minimizes its electronic influence on reactivity at the metal center. Steric differences from triphenylphosphine are also minimal: the cone angle of *meta*-triphenyl phosphine monosulfonate is similar to that of triphenylphosphine (151° and 145°, respectively).[53,54] In solution TPPMS is well known to bind to the metal through phosphorus and not the sulfonate group. ^{31}P NMR experiments for various Au^{I}(TPPMS)L complexes in D_2O and CD_3OD confirm this showing singlet signals at approximately 37 ppm compared to the signal for free TPPMS which is around −6 ppm.[55]

To further confirm the binding mode of TPPMS to $CH_3CO_2M^{I}$ (M = Cu, Ag, Au), we have calculated the two isomeric structures **A** and **B** for each complex, **1(a-c)**, in the gas phase and in water and methanol. Table 1 shows that the complexes are most stabilized by methanol, and as expected, binding through phosphorus is strongly favored in both methanol and water. In the gas phase the binding preference is reversed for copper and silver both of which favor binding through one of the oxygen atoms of the sulfonate group. However, the difference in energies between binding modes only minimally favors oxygen binding: 0.08 eV for copper and 0.05 eV for silver. Gold continues to strongly favor binding through phosphorus even in the gas phase (by 0.60 eV).

Although, in the case of copper and silver, binding to the metal *via* the sulfonate group is theoretically favored in the gas phase, it is likely that we do not observe this O-bound complex. Instead, since the metal complexes are initially formed in solution and gently transferred into the gas phase *via* electrospray ionization, and there is likely a high energy barrier to isomerization between the two forms, the P-bound complex is expected to be preserved. This assumption is consistent with experimental data: if the ligand was bound through the sulfonate group we would expect to observe desulfonation of the ligand (−80 Da) as one of the fragmentation pathways,[33] but no such fragmentation pathway was detected in the copper or silver systems.

Table 1 A theoretical comparison of the relative energies of isomeric structures in which TPPMS binds *via* either the P or O atoms to the coinage metal acetates in methanol, water and the gas phase. Entries are reported in eV and are relative to the case where phosphorus binds to the given metal in methanol (bold entries). In addition, relative stabilities of the isomers in water and in the gas phase are given in parentheses

Isomer A: Bound through P

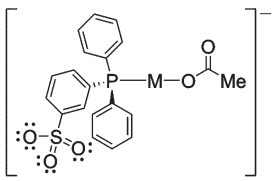

Isomer B: Bound through O

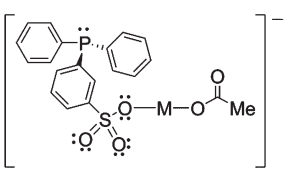

Metal	Isomer	Methanol	Water	Gas
Cu^{I}	**A**	**0.00**	0.06(0.00)	3.44(0.08)
	B	0.51	0.59(0.53)	3.36(0.00)
Ag^{I}	**A**	**0.00**	0.06(0.00)	3.35(0.05)
	B	0.62	0.72(0.66)	3.30(0.00)
Au^{I}	**A**	**0.00**	0.07(0.00)	3.20(0.00)
	B	1.20	1.30(1.23)	3.80(0.60)

2. Gas-phase fragmentation reactions of M^{I}(TPPMS) complexes

Negative-ion electrospray ionisation of a methanolic solution of the appropriate metal acetate, [PPN][TPPMS], and the appropriate carboxylic acid resulted in the observation of a range of anions including $[(TPPMS)M^{I}O_2CR]^-$ where M = Cu, Ag, or Au and R = Me, Et, benzyl or Ph (see ESI Fig. 1–12† for the full ESI mass spectrum for each of the 12 solutions). Each of the complexes, $[(TPPMS)M^{I}O_2CR]^-$, were isolated within a linear ion trap mass spectrometer in the gas phase and subjected to collision-induced dissociation (CID) in order to investigate their unimolecular chemistry. In all cases a monoisotopic signal containing ^{63}Cu, ^{107}Ag or ^{197}Au (the lightest and most abundant isotopomer for each of the copper silver and gold complexes, respectively) was isolated from the isotope pattern of interest for further experimentation.

2.1. Gas-phase fragmentation of $[(TPPMS)Cu^{I}O_2CR]^-$ and $[(TPPMS)Cu^{I}R]^-$. Fig. 1 shows the MS^2 CID spectrum for each of the copper complexes, $[(TPPMS)Cu^{I}O_2CR]^-$, where R = Me (*m*/*z* 463, **1a**), R = Et (*m*/*z* 477, **2a**), R = benzyl (*m*/*z* 539, **3a**) and R = Ph (*m*/*z* 525, **4a**).

It is apparent from Fig. 1 that ions **1a–4a** decompose by a common set of competing fragmentation pathways, namely decarboxylation (eqn (1), M = Cu, signals at *m*/*z* 419, 433, 495 and 481, respectively for complexes **1a–4a**), loss of the phosphine ligand (eqn (2), M = Cu, signal at *m*/*z* 341), or loss of the carboxylic acid (eqn (3), M = Cu, signal at *m*/*z* 403). Loss of the carboxylic acid presumably arises from initial orthometallation and deprotonation of the phosphine ligand assisted by the carboxylato ligand, and this type of reactivity has precedence in the literature.[56,57] Since the neutral products are not detected in our experiments, we cannot rule out a second pathway in which decarboxylation occurs first followed closely by loss of

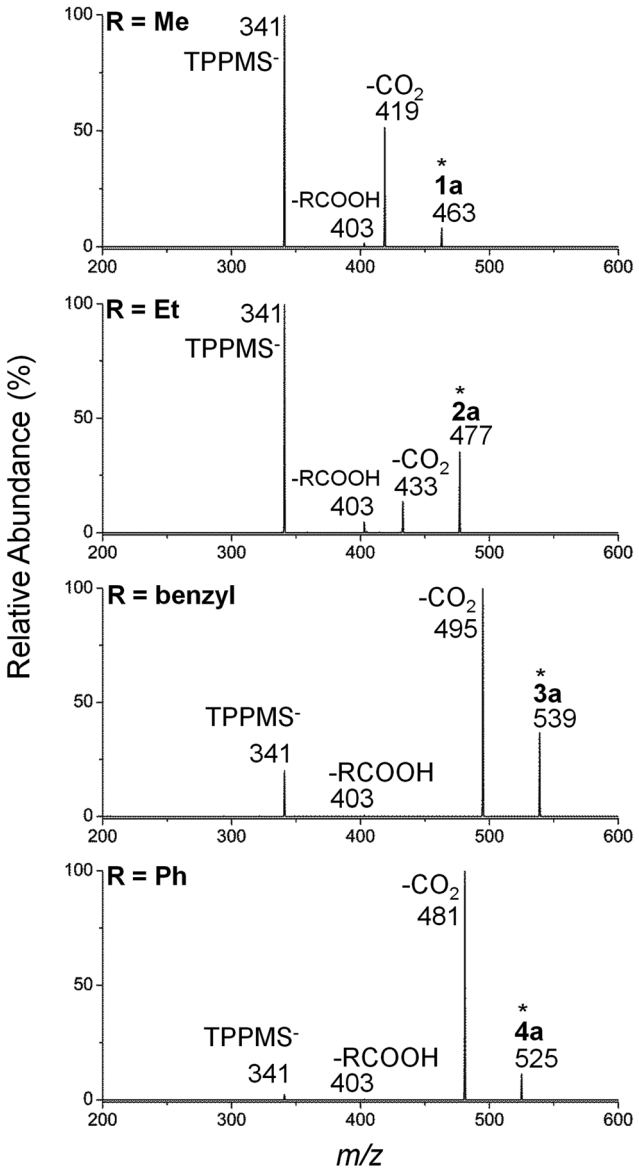

Fig. 1 LTQ MS^2 CID spectra for copper complexes **1a–4a**. The mass selected precursor ion is marked with a star (*).

RH to give an overall loss of [R,C,H,O_2]. Finally, loss of the carboxylato ligand as the carboxylate (eqn (4)) was hypothesized as a possible fragmentation pathway based on evidence in earlier work performed on $[(R^1)Cu^I(O_2CR^2)]^-$ complexes which do not bear a phosphine ligand,[26] but no such loss was observed for any of the ions in this work.

$$[(\mathrm{TPPMS})^{\mathrm{I}}\mathrm{MO_2CR}]^- \rightarrow [(\mathrm{TPPMS})\mathrm{M^IR}]^- + \mathrm{CO_2} \quad (1)$$

$$\rightarrow \mathrm{M^IO_2CR} + [\mathrm{TPPMS}]^- \quad (2)$$

$$\rightarrow [(\mathrm{TPPMS\text{-}H})\mathrm{M^I}]^- + [\mathrm{R,C,H,O_2}] \quad (3)$$

$$\rightarrow (\mathrm{TPPMS})\mathrm{M^I} + [\mathrm{RCO_2}]^- \quad (4)$$

The relative signal intensities corresponding to each of the fragmentation pathways 1–3 suggest that decarboxylation (eqn (1)) is favoured for complexes **3a** and **4a**, while phosphine ligand loss (eqn (2)) is the favoured pathway for complexes **1a** and **2a**. In all cases acid loss is a minor channel. It should be noted that while these signal intensities can provide a general indication of which fragmentation pathway is favoured over the others, they do not provide a quantitative measure of the relative energies of the fragmentation pathways. This issue is addressed by performing energy-dependent CID experiments and a quantitative discussion on which pathways are favoured for a given complex is discussed in Section 3.

A very small signal was observed for bond homolysis in the MS/MS spectrum of **2a** (eqn (5)) and this was the only other fragmentation pathway observed on CID of complexes **1a–4a**.

$$[(\mathrm{TPPMS})\mathrm{Cu^IO_2CCH_2CH_3}]^- \rightarrow [(\mathrm{TPPMS})\mathrm{Cu}]^{\cdot -} + [\mathrm{C_3,H_5,O_2}]^{\cdot} \quad (5)$$

Subsequent isolation of the decarboxylated product ion $[(\mathrm{TPPMS})\mathrm{Cu^IR}]^-$ followed by CID overwhelmingly resulted in loss of the phosphine ligand (eqn (6), M = Cu, *m/z* 341) for all R groups (see ESI Fig. 13–16†). In all cases a very small signal was also observed for loss of RH (eqn (7)) once again indicating deprotonation of the phosphine ligand.

$$[(\mathrm{TPPMS})\mathrm{M^IR}]^- \rightarrow \mathrm{M^IR} + [\mathrm{TPPMS}]^- \quad (6)$$

$$\rightarrow [(\mathrm{TPPMS\text{-}H})\mathrm{M^I}]^- + \mathrm{RH} \quad (7)$$

In the case of $[(\mathrm{TPPMS})\mathrm{Cu^ICH_2CH_3}]^-$ (**2a**) another signal is observed for loss of C_2H_4 which is indicative of β-hydride elimination (eqn (8)) and similar reactivity has been observed in previous gas-phase work.[26,27]

$$[(\mathrm{TPPMS})\mathrm{Cu^ICH_2CH_3}]^- \rightarrow [(\mathrm{TPPMS})\mathrm{Cu^IH}]^- + (\mathrm{C_2H_4}) \quad (8)$$

2.2. Gas-phase fragmentation of $[(\mathrm{TPPMS})\mathrm{Ag^IO_2CR}]^-$ and $[(\mathrm{TPPMS})\mathrm{Ag^IR}]^-$. Fig. 2 shows the MS^2 CID spectrum for each of the silver complexes, $[(\mathrm{TPPMS})\mathrm{Ag^IO_2CR}]^-$, where R = Me (*m/z* 507, **1b**), Et (*m/z* 521, **2b**), benzyl (*m/z* 583, **3b**) and Ph (*m/z* 569, **4b**).

The silver complexes fragment by the same three fragmentation pathways as the copper complexes. Signals are observed for: decarboxylation (eqn (1), M = Ag, signals at *m/z* 463, 477, 539 and 525, respectively for complexes **1b–4b**), loss of the phosphine ligand (eqn (2), M = Ag, signal at *m/z* 341), and acid loss (eqn (3), M = Ag, signal at *m/z* 447). For all silver systems, the pathway for loss of the phosphine ligand is the dominant signal and acid loss is a very minor channel. The decarboxylation channel is highly dependent on the nature of the R group.

Isolation and subsequent CID of the decarboxylated silver complexes $[(\mathrm{TPPMS})\mathrm{Ag^I(R)}]^-$ resulted exclusively in loss of the phosphine ligand (eqn (6), M = Ag, *m/z* 341) for all R groups except R = Et (**2b**) (see ESI Fig. 17–20†). In the case of R = Et the decarboxylated product $[(\mathrm{TPPMS})\mathrm{Ag^ICH_2CH_3}]^-$ (**2b**) was too low in intensity to isolate.

2.3. Gas-phase fragmentation of $[(\mathrm{TPPMS})\mathrm{Au^IO_2CR}]^-$ and $[(\mathrm{TPPMS})\mathrm{Au^IR}]^-$. Fig. 3 shows the MS^2 CID spectrum for each

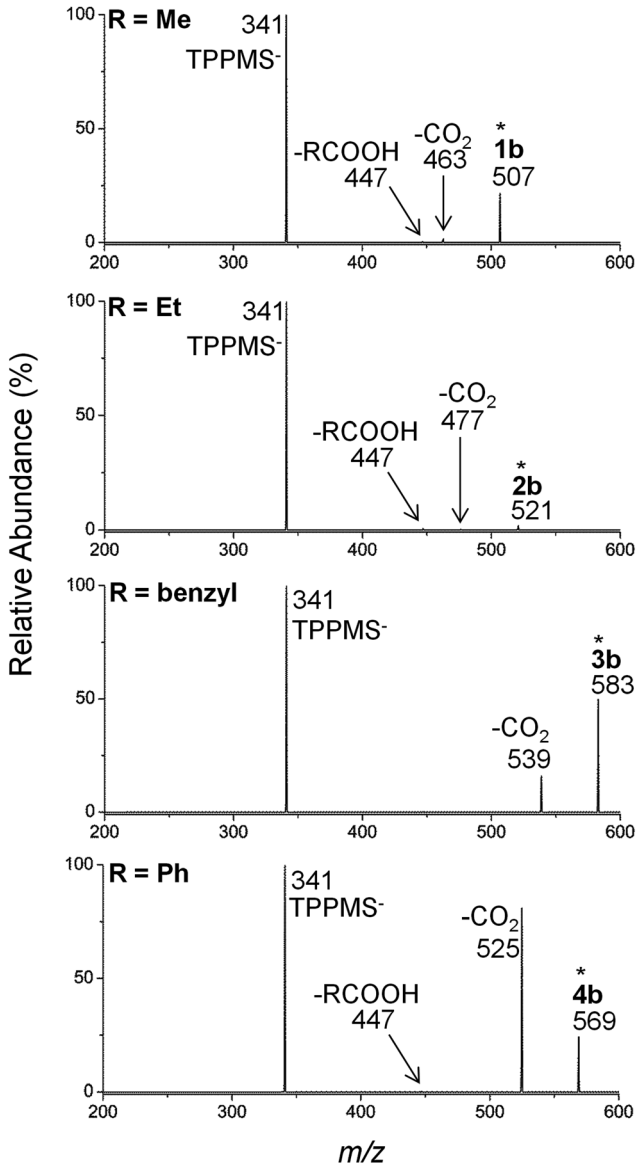

Fig. 2 LTQ MS^2 CID spectra for silver complexes **1b–4b**. The mass selected precursor ion is marked with a star (*).

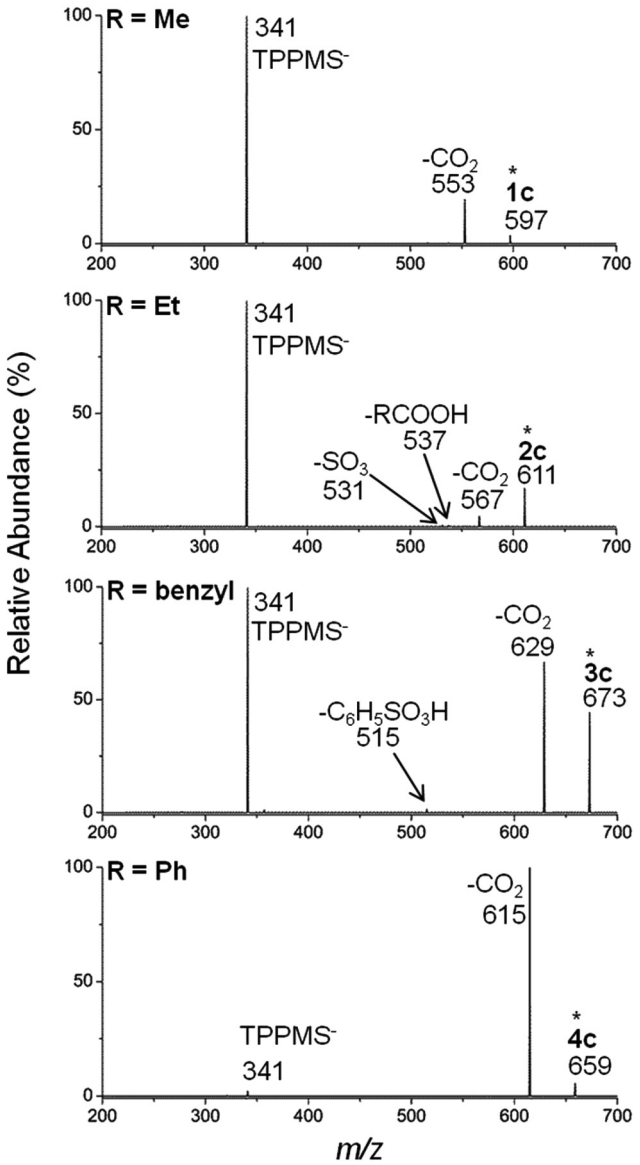

Fig. 3 LTQ MS^2 CID spectra for gold complexes **1c–4c**. The mass selected precursor ion is marked with a star (*).

of the gold complexes, $[(TPPMS)Au^{I}O_2CR]^-$, where R = Me (*m/z* 597, **1c**), Et (*m/z* 611, **2c**), benzyl (*m/z* 673, **3c**) and Ph (*m/z* 659, **4c**).

Once again major fragmentation pathways were observed for: decarboxylation (eqn (1), M = Au, signals at *m/z* 553, 567, 629 and 615 for complexes **1c–4c**, respectively); loss of the phosphine ligand (eqn (2), M = Au, signal at *m/z* 341); and acid loss (eqn (3), M = Au, signal at *m/z* 537 for complexes **1c** and **2c** only). Loss of the phosphine ligand is dominant for all gold complexes except R = Ph (**4c**) where decarboxylation almost completely replaces phosphine loss. Acid loss is only observed for R = Me (**1c**) and Et (**2c**) and is a very minor channel. The relative intensity of the decarboxylation channel is again highly dependent on R. Two other minor reaction channels were observed that were not present in the copper and silver systems: (1) loss of SO_3 (eqn (9), *m/z* 531) from $[(TPPMS)Au^{I}(O_2CEt)]^-$ (**2c**) and, (2) loss of a fragment with the stoichiometry $[C_6,H_6,S,O_3]$ (eqn (10), *m/z* 515) from $[(TPPMS)Au^{I}(O_2CCH_2Ph)]^-$ (**3c**).

$$[(TPPMS)Au^{I}CO_2CH_2CH_3]^- \rightarrow [(TPPMS\text{-}SO_3)Au^{I}CO_2CH_2CH_3]^- + SO_3 \quad (9)$$

$$[(TPPMS)Au^{I}CO_2CH_2Ph]^- \rightarrow [(TPPMS\text{-}C_6H_6SO_3)Au^{I}CO_2CH_2Ph]^- + [C_6, H_6, S, O_3] \quad (10)$$

Isolation and subsequent CID of the decarboxylated gold complexes $[(TPPMS)Au^{I}(R)]^-$ resulted exclusively in loss of the phosphine ligand (eqn (6), M = Au, *m/z* 341) (see ESI Fig. 21–24†).

3. Energy-resolved CID experiments

While indirect information on the relative energies of various fragmentation pathways can be estimated based on the LTQ CID experiments, a more quantitative measure can be achieved by performing energy-dependent CID experiments using a Q-TOF instrument. Accordingly, energy-dependent CID experiments were performed on all complexes **1(a-c)–4(a-c)** to probe the relative energies required for decarboxylation (eqn (1)), loss of the phosphine ligand (eqn (2)) and loss of the acid (eqn (3)) for each combination of metal (Cu, Ag, Au) and R group (Me, Et, benzyl, Ph). Solutions identical to those prepared for the LTQ experiments were electrosprayed in the negative-ion mode and a monoisotopic signal containing ^{63}Cu, ^{107}Ag or ^{197}Au (for copper, silver and gold complexes, respectively) was isolated from the isotope pattern of interest for fragmentation in the collision cell. The collision energy was increased from 0 V to 40 V in increments of 1 V and an MS^2 spectrum was recorded at each collision energy. Fig. 4 shows a representative plot of the type of data obtained, which is displayed in two different ways. On the top, a single mass spectrum shows the summed intensities of the observed ions from all MS^2 spectra collected over the range of collision energies and conveys the overall intensity of each signal. On the bottom is an energy-resolved plot with *m*/*z* on the *x*-axis, collision energy on the *y*-axis and relative signal intensity, shown as contours, on the *z*-axis (the contours are too small to be seen in the current view). In this second format the individual MS^2 spectra collected at each collision energy are "stacked" one on top of the other along the *y*-axis going from a collision voltage of 0 V to 40 V. The lines in the plot correspond to the ions in the summed spectrum above and indicate at which collision energies those ions are experimentally observed. Thus, this plot allows a direct measure of the relative energy required to activate a given fragmentation pathway.

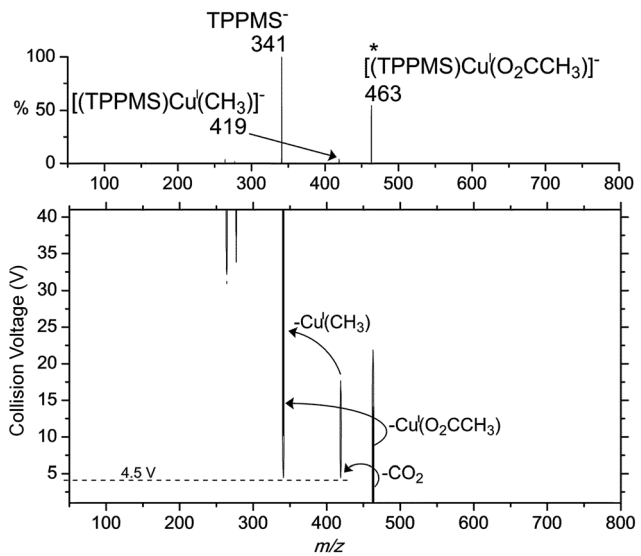

Fig. 4 Energy-dependent CID plot of **1a**. The mass selected precursor ion is marked in the top spectrum by a star (*).

The intensity threshold for displaying a signal in the energy-resolved plot is arbitrarily set at 2% relative to the initial intensity of the precursor ion.

On examination of the energy-dependent fragmentation of complex **1a** in Fig. 4, we can observe that the decarboxylation (*m*/*z* 419) and loss of the phosphine ligand (*m*/*z* 341) fragmentation pathways are energetically competitive: the signals representing each pathway in the bottom plot are observed to appear beginning at a collision voltage of approximately 4.5 V. The signal for loss of the acid (eqn (3)) never exceeds the set 2% threshold in the energy-resolved plots and therefore this pathway does not register in the lower plot (this holds true for all complexes investigated in this work).

A qualitative comparison of the LTQ CID data for complex **1a** (top of Fig. 1) with the summed CID data from the Q-TOF for **1a** (top of Fig. 4) does not yield a good match. Specifically, the summed Q-TOF data shows a very strong signal for loss of the phosphine ligand. This effect is observed in all of the summed Q-TOF data. It reflects the fact that at high collision energies loss of the phosphine ligand occurs not only from the reactant ion but also from the decarboxylated product ion (eqn (6), the LTQ CID experiments on $[(TPPMS)M^{I}(R)]^{-}$ confirm this) and at very high collision energies $[TPPMS]^{-}$ is the only surviving ion. The LTQ data, on the other hand, was collected at a single collision energy selected to best represent all fragmentation pathways. Consequently, the relative intensity of the signal for loss of the phosphine ligand in the summed Q-TOF data is deceivingly large when compared to the signal for decarboxylation and it should not be used for comparison. Conversely, the summed intensity for decarboxylation over all collision energies as compared to the summed intensity of the reactant ion over all collision energies for the Q-TOF data *is* a useful measure and it is discussed in detail ahead.

Plots such as the one in Fig. 4 are available in the ESI (ESI Fig. 25–35†) for each of the complexes $[(TPPMS)M^{I}(O_2CR)]^{-}$ and are summarized here. Three pieces of information are extracted from the energy-resolved CID experiments: (1) the summed intensity of the decarboxylation fragmentation channel over all collision energies relative to the intensity of the reactant ion summed over all collision energies; (2) the lowest collision energy required for loss of the phosphine ligand; and (3) the lowest collision energy required for decarboxylation. These data allow us to answer two questions. First, which metals and which R groups, or combinations thereof, best facilitate decarboxylation? Second, how do the relative energies for loss of the phosphine ligand and decarboxylation compare for a given combination of M and R?

The first question is answered by plotting the ratio of the decarboxylated product ion to the selected reactant ion from the summed energy-resolved plot for each complex $[(TPPMS)M^{I}(O_2CR)]^{-}$ (Fig. 5). This allows us to determine which complexes are best at facilitating decarboxylation of the carboxylate ligand.

From Fig. 5 we see that in general copper is best at facilitating decarboxylation, followed by gold and then silver. The one exception to this trend is when R = Ph and M = Au which has a

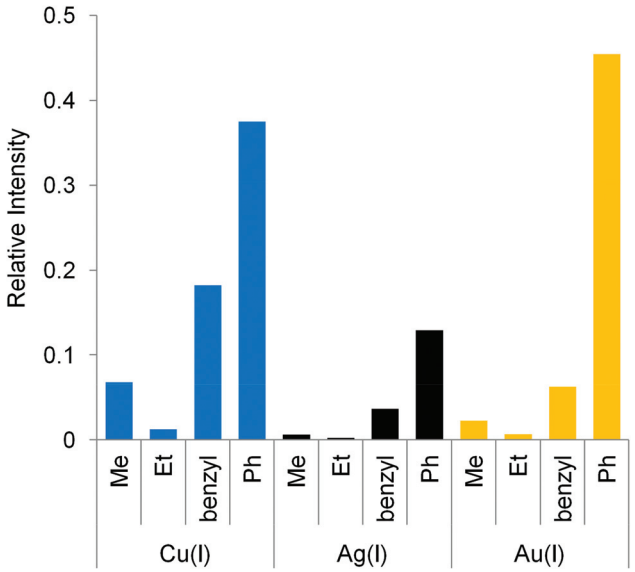

Fig. 5 A comparison of decarboxylation ability for the complexes [(TPPMS)$M^{I}(O_2CR)]^-$ (M = Cu, Ag, Au. R = Me, Et, Ph, benzyl). Relative intensity on the *y*-axis is the ratio of the signal intensity of the decarboxylated product ion summed over collision energies 0–40 V from the energy-resolved CID experiments divided by the signal intensity of the reactant ion summed over collision energies 0–40 V from the same experiment.

higher-than-expected propensity for decarboxylation. Ph is by far the best of the R groups studied in this work for facilitating decarboxylation, followed by R = benzyl, R = Me and finally R = Et. The relative intensity of the various fragmentation pathways as measured by the LTQ CID experiments qualitatively follow the same trends that are observed in the Q-TOF data displayed in Fig. 5. The high propensity for the M = Au, R = Ph system to facilitate decarboxylation is consistent with recent studies on gold(I)-facilitated decarboxylations of aromatic carboxylates in the condensed phase which also found that gold decarboxylated these substrates more easily than silver or copper.[20,21]

The second question, posed above, is answered by comparing the lowest collision energy required to observe the decarboxylation channel with the lowest collision energy required to observe the loss of the phosphine ligand channel. Table 2 summarizes this data. For the majority of metal/R group combinations the energy required for loss of the phosphine ligand is lower than that for decarboxylation and thus, loss of the phosphine ligand is favoured. The one exception to this observation (that is true for all three metals) is when R = Ph.

From Table 2 we can also see that the energy required for loss of the phosphine ligand increases in the order Ag < Cu < Au, and this is discussed further in Section 4.

4. DFT calculations on the competition between decarboxylation and ligand loss

DFT calculations were performed to gain additional insight into the observed experimental reactivity. The lowest energy

Table 2 Collision energies (V) required for decarboxylation and loss of the phosphine ligand reactions for $[LM^{I}O_2CR]^-$ (where L = TPPMS)

M =; R =	$[LM^{I}O_2CR] + CO_2$ [a] (eqn (1))	$L^- + [M^{I}O_2CR]$[a] (eqn (2))	Decarboxylation favoured?
Cu; Me	4.5	4.5	No
Cu; Et	N/A	7.0	No
Cu; $PhCH_2$	5.3	8.0	Yes
Cu; Ph	3.4	8.0	Yes
Ag; Me	N/A	1.0	No
Ag; Et	N/A	2.0	No
Ag; $PhCH_2$	6.3	4	No
Ag; Ph	2.5	3.7	Yes
Au; Me	9.7	6.5	No
Au; Et	N/A	10.0	No
Au; $PhCH_2$	10.8	9.0	No
Au; Ph	3.8	8.5	Yes

[a] Indicates the collision energy (V) at which the product ion signal reaches 2% relative to the initial intensity of the reactant ion.

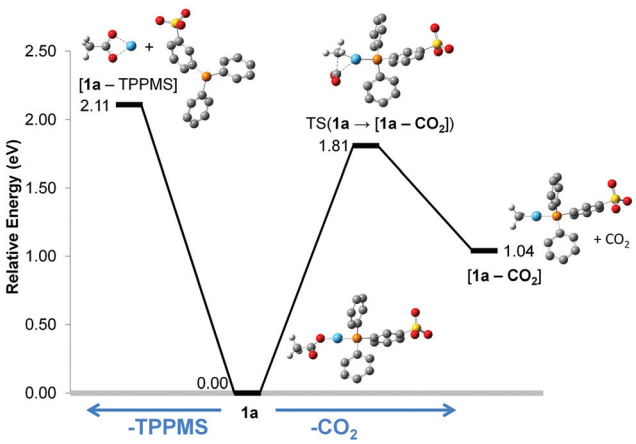

Fig. 6 Potential energy diagram including optimized structures for loss of the phosphine ligand from **1a** (left) and decarboxylation from **1a** (right). Energies given are electronic energies + zero point energy.

pathways for decarboxylation and loss of the phosphine and carboxylato ligands were calculated for each of the twelve complexes **1(a-c)**–**4(a-c)**. Fig. 6 shows the relevant optimized structures and potential energy diagram for [(TPPMS)-$Cu^{I}(O_2CCH_3)]^-$ (**1a**).

The optimized structures shown for **1a** are representative of those calculated for the other complexes (see ESI Fig. 36–47†). For all complexes, the carboxylato ligand binds in an η^1-fashion, forming a linear geometry at the metal center. η^1-Binding of carboxylates to phosphine-ligated copper has been observed experimentally by IR[58] and X-ray crystallography[59,60] and is proposed to be primarily an electronic and not a steric effect in which carboxylates with electron-withdrawing substituents more strongly favour monodentate binding. Consistent with previous work on the coinage metal complexes $[CH_3CO_2M^{I}O_2CR]^-$,[26,27,30] decarboxylation occurs *via* a concerted 3-centered transition state to release CO_2 and

Table 3 DFT-predicted energies for competing decarboxylation (eqn (1)), loss of the phosphine ligand (eqn (2)) and carboxylate anion loss (eqn (4)) reactions for $[LMO_2CR]^-$ (where L = TPPMS)

M = ; R =	$[LM^IR] + CO_2$[a] (eqn (1))	$L^- + [M^IO_2CR]$[b] (eqn (2))	$[LM^I] + RCO_2^-$[b] (eqn (4))	Decarboxylation favoured?
Cu; Me	1.81(1.04)	2.11	4.17	Yes
Cu; Et	1.91(1.24)	2.12	4.15	Yes
Cu; $PhCH_2$	1.70(0.83)	2.15	3.94	Yes
Cu; Ph	1.67(1.11)	2.15	3.96	Yes
Ag; Me	1.71(0.80)	1.69	3.63	No
Ag; Et	1.80(0.97)	1.67	3.59	No
Ag; $PhCH_2$	1.61(0.60)	1.71	3.40	Yes
Ag; Ph	1.50(0.91)	1.73	3.42	Yes
Au; Me	1.92(0.37)	2.83	3.82	Yes
Au; Et	2.00(0.54)	2.86	3.80	Yes
Au; $PhCH_2$	1.90(0.24)	2.86	3.59	Yes
Au; Ph	1.48(0.47)	2.90	3.60	Yes

[a] Activation energy (eV) for decarboxylation reactions. The values in parenthesis refer to the overall endothermicity of the reaction. [b] Reaction endothermicity (eV) for carboxylate anion loss (assumed as barrierless).

afford a new metal–carbon bond (TS(**1a** → [**1a**–CO_2]) in Fig. 6). Loss of the phosphine ligand was assumed to be barrierless. The energies associated with decarboxylation, phosphine ligand loss and loss of the carboxylate for each complex **1(a-c)–4(a-c)** are summarized in columns two, three and four of Table 3, respectively.

A comparison of the first column in Table 3 with Fig. 5 shows good agreement between theory and experiment with regard to the relative ease of decarboxylation for a given R group. Indeed, a graphical comparison of the experimentally determined ease of decarboxylation *versus* the calculated transition state energy for decarboxylation indicates that overall, as expected, less of the decarboxylation product is observed for systems with a higher calculated transition state energy (ESI Fig. 37†). Theory and experiment both indicate that R = Ph is best at facilitating decarboxylation followed by R = benzyl, Me and Et for all of the metals Cu, Ag and Au. This may be due to the strength of the resulting metal–R group bond: the calculated M–R bonds in $[(TPPMS)M^I(R)]^-$ are shortest when R = Ph for a given metal. Theory also predicts that the combination M = Au and R = Ph will provide the best conditions for decarboxylation. Where theoretical calculations fail is in the relative ability of the different metals to facilitate decarboxylation. Theory predicts that in general silver will be better than copper and gold, when in fact experimental results prove silver to be the least active towards decarboxylation. Condensed-phase work on decarboxylation of aromatic carboxylates agrees with theory by observing that a lower temperature is required to facilitate decarboxylation in solution using a silver-based catalyst as compared to a copper-based catalyst.[17,18] The origin of the low reactivity of silver towards decarboxylation in the gas phase is unclear, but it is consistent for all R-groups tested here and previous gas-phase work has also observed silver to be inferior to copper in facilitating decarboxylation.[27]

As noted in the previous section, energy-resolved CID experiments performed on the Q-TOF instrument indicate that the energy required for loss of the phosphine ligand increases in the order Ag < Cu < Au. This is consistent with the calculated energies for ligand loss shown in column three Table 3 (eqn (2)). The same trend was observed in other work for the binding energies in MPH_3 (M = Cu, Ag, Au) as determined from high-level CCSD(T) calculations performed by Granatier *et al.*[61]

A comparison of the last column in Tables 2 and 3 reveals that theory predicts decarboxylation should be favoured much more than we see experimentally. The origin of this discrepancy is that theory overestimates the energy for loss of the phosphine ligand. This can be explained by the fact that CID is effectively a heating process and loss of the phosphine ligand is favoured at increased temperatures since it is entropically preferred over decarboxylation. This is not accounted for in the calculations since all structures were calculated at 25 °C.

Carboxylate anion loss (eqn (4)) has been a commonly observed pathway in much of our other work on decarboxylation reactions with coinage metals, so the energy required for carboxylate anion loss from complexes **1(a-c)–4(a-c)** was also calculated. These values are listed in the fourth column of Table 3. As mentioned in Section 2.1 carboxylate anion loss is not observed experimentally for any of the systems **1(a-c)–4(a-c)** and theory clearly shows that this pathway is indeed energetically unfavourable. This is in sharp contrast to coinage metal complexes not bearing a phosphine ligand and we discuss this further in Section 5.

5. Comparison with the gas-phase reactivity of metal carboxylates not bearing a phosphine ligand

Since the gas-phase unimolecular chemistry of $[LM^IO_2CCH_3]^-$ has been studied for M = Cu, Ag, Au where L = Me,[26,27,30] we are able to compare trends in their formation and reactivity with the analogous complexes $[LM^IO_2CCH_3]^-$ where L = TPPMS. The same level of theory and basis set was used in previous work and in this work, thus theoretical results for the two families of complexes are also compared here. Overall, we observe that substitution of the anionic methyl ligand for a neutral donor phosphine ligand (bearing an ancillary charged group) results in markedly different unimolecular reactivity.

For the complexes studied in previous works, $[CH_3M^IO_2CCH_3]^-$ (M = Cu, Ag, Au), decarboxylation is the strongly favoured fragmentation pathway both in experiment and theory (eqn (11), L = Me, 1.67 eV (Cu), 1.66 eV (Ag) and 1.65 eV (Au)), and while direct observation of ligand loss ($-Me^-$) cannot be observed due to the low mass cut-off of the mass spectrometer, this pathway (eqn (12), L = Me) is calculated to be much higher in energy than decarboxylation (4.36 eV (Cu), 4.05 eV (Ag), and 5.33 eV (Au)). In contrast, the complexes $[(TPPMS)M^IO_2CCH_3]^-$ fragment predominantly *via* TPPMS ligand loss (eqn (12), L = TPPMS) and decarboxylation (eqn (11), L = TPPMS) is a less favoured pathway (see Table 3 and

Section 4 of this work for discussion of the predicted energies for these pathways). DFT calculations suggest that this is primarily due to the fact that TPPMS has a lower binding energy than Me and not because the pathway for decarboxylation is significantly lower in energy when L = Me.

$$[LM^{I}O_2CCH_3]^- \rightarrow [LM^{I}CH_3]^- + CO_2 \quad (11)$$

$$\rightarrow M^{I}O_2CCH_3 + [L]^- \quad (12)$$

$$\rightarrow LM^{I} + [CH_3CO_2]^- \quad (13)$$

DFT calculations predict another viable fragmentation pathway for the methyl-ligated complexes $[CH_3M^{I}O_2CCH_3]^-$ (M = Cu, Ag, Au) that is energetically competitive with decarboxylation, specifically: carboxylate anion loss (eqn (13), L = Me, 1.86 eV (Cu), 1.68 eV (Ag) and 1.72 eV (Au)). Experimental results confirm that this fragmentation channel is active on CID of the complexes $[CH_3M^{I}O_2CCH_3]^-$ where M = Cu and Ag but not where M = Au. On the other hand, DFT calculations indicate that carboxylate anion loss (eqn (4)) is prohibitively high in energy for the phosphine-ligated complexes $[(TPPMS)M^{I}O_2CR]^-$ (M = Cu, Ag, Au) (4.17 eV (Cu), 3.63 eV (Ag) and 3.82 eV (Au)). The absence of a signal for this pathway (at *m*/*z* 59) in the Q-TOF experimental data (which has a low mass cut-off of *m*/*z* 50) provides further confirmation that carboxylate anion loss does not occur when L = TPPMS.

Conclusions

Here we have extended the decarboxylation strategy developed for copper, silver and gold carboxylates complexes of the type $[RCO_2M^{I}L]^-$ to complexes where L is a fixed-charge phosphine ligand. We find that: (1) the energy required for loss of the phosphine ligand in the gas phase is lowest for silver, then copper, and highest for gold. (2) Of the tested R groups, Ph is by far the best at facilitating decarboxylation in the gas phase, followed by R = benzyl, R = Me and finally R = Et. This preference for decarboxylation from sp^2-hybridized carbon centers has been observed in our previous gas-phase studies and is a common theme in condensed-phase work. (3) In general, copper(I) is best at facilitating decarboxylation in the gas phase, followed by gold(I) then silver(I). The one exception to this trend is when R = Ph and M = Au which has the highest overall propensity for decarboxylation. This combination of R = Ph and M = Au has also been shown to be particularly good at decarboxylation in the condensed phase.[20,21]

In comparison to previous gas-phase studies, we find that use of a phosphine ligand favors decarboxylation by dramatically reducing the availability of the fragmentation pathway for carboxylate anion loss, which in non-phosphine-containing metal carboxylates lowers the efficiency of decarboxylation. However, ligand loss becomes competitive with decarboxylation for phosphine-containing metal carboxylates, and in most cases loss of the phosphine ligand is the most favoured fragmentation channel.

Acknowledgements

We thank the ARC for financial support *via* grants DP110103844 (to RAJO and GNK) and DP1096134 (GNK). We thank the Victorian Partnership for Advanced Computing and the University of Melbourne for generous allocation of computer time. JSM thanks the CFI and BCKDF for infrastructure support and the NSERC for operational funding (Discovery and Discovery Accelerator Supplement). We thank Dr Gabriel da Silva for helpful discussions.

References

1 L. J. Gooßen, K. Gooßen, N. Rodriguez, M. Blanchot, C. Linder and B. Zimmermann, *Pure Appl. Chem.*, 2008, **80**, 1725.
2 L. J. Gooßen, N. Rodriguez and K. Gooßen, *Angew. Chem., Int. Ed.*, 2008, **47**, 3100.
3 J. D. Weaver, A. Recio, A. J. Grenning and J. A. Tunge, *Chem. Rev.*, 2011, **111**, 1846.
4 N. Rodríguez and L. J. Goossen, *Chem. Soc. Rev.*, 2011, **40**, 5030.
5 R. Shang and L. Liu, *Sci. China Chem.*, 2011, **54**, 1670.
6 J. Cornella and I. Larrosa, *Synthesis*, 2012, 653.
7 A. F. Shepard, N. R. Winslow and J. R. Johnson, *J. Am. Chem. Soc.*, 1930, **52**, 2083.
8 M. Nilsson, *Acta Chem. Scand.*, 1966, **20**, 423.
9 M. Nilsson and C. Ullenius, *Acta Chem. Scand.*, 1968, **22**, 1998.
10 J. Chodowska-Palicka and M. Nilsson, *Acta Chem. Scand.*, 1970, **44**, 3353.
11 T. Cohen and R. A. Schambach, *J. Am. Chem. Soc.*, 1970, **92**, 3189.
12 T. Cohen, R. W. Berninger and J. T. Wood, *J. Org. Chem.*, 1978, **43**, 837.
13 A. Cairncross, J. R. Roland, R. M. Henderson and W. A. Sheppard, *J. Am. Chem. Soc.*, 1970, **92**, 3187.
14 L. J. Goossen, W. R. Thiel, N. Rodriguez, C. Linder and B. Melzer, *Adv. Synth. Catal.*, 2007, **349**, 2241.
15 L. J. Goossen, F. Manjolinho, B. A. Khan and N. Rodriguez, *J. Org. Chem.*, 2009, **74**, 2620.
16 R. Shang, Y. Fu, Y. Wang, Q. Xu, H.-Z. Yu and L. Liu, *Angew. Chem., Int. Ed.*, 2009, **48**, 9350.
17 L. J. Goossen, C. Linder, N. Rodriguez, P. P. Lange and A. Fromm, *Chem. Commun.*, 2009, 7173.
18 J. Cornella, C. Sanchez, D. Banawa and I. Larrosa, *Chem. Commun.*, 2009, 7176.
19 P. Lu, C. Sanchez, J. Cornella and I. Larrosa, *Org. Lett.*, 2009, **11**, 5710.
20 S. Dupuy, F. Lazreg, A. M. Z. Slawin, C. S. J. Cazin and S. P. Nolan, *Chem. Commun.*, 2011, **47**, 5455.
21 J. Cornella, M. Rosillo-Lopez and I. Larrosa, *Adv. Synth. Catal.*, 2011, **353**, 1359.
22 R. A. J. O'Hair, *Chem. Commun.*, 2006, 1469.

23 R. A. J. O'Hair, in *MS investigations of reactive intermediates in solution*, ed. L. S. Santos, Wiley-VCH, Weinheim, 2010, ch. 6, pp. 199–227.
24 R. A. J. O'Hair, *Chem. Commun.*, 2002, 20.
25 P. F. James and R. A. J. O'Hair, *Org. Lett.*, 2004, **6**, 2761.
26 N. Rijs, T. Waters, G. N. Khairallah and R. A. J. O'Hair, *J. Am. Chem. Soc.*, 2008, **130**, 1069.
27 N. J. Rijs and R. A. J. O'Hair, *Organometallics*, 2009, **28**, 2684.
28 N. J. Rijs, B. F. Yates and R. A. J. O'Hair, *Chem.–Eur. J.*, 2010, **16**, 2674.
29 N. J. Rijs and R. A. J. O'Hair, *Organometallics*, 2010, **29**, 2282.
30 N. J. Rijs, G. B. Sanvido, G. N. Khairallah and R. A. J. O'Hair, *Dalton Trans.*, 2010, **39**, 8655.
31 N. J. Rijs, N. Yoshikai, E. Nakamura and R. A. J. O'Hair, *J. Am. Chem. Soc.*, 2012, **134**, 2569.
32 N. J. Rijs and R. A. J. O'Hair, *Dalton Trans.*, 2012, **41**, 3395.
33 L. O. Sraj, G. N. Khairallah, G. da Silva and R. A. J. O'Hair, *Organometallics*, 2012, **31**, 1801.
34 M. I. S. Röhr, J. Petersen, C. Brunet, R. Antoine, M. Broyer, P. Dugourd, V. Bonačić-Koutecký, R. A. J. O'Hair and R. Mitrić, *J. Phys. Chem. Lett.*, 2012, **3**, 1197.
35 N. J. Rijs and R. A. J. O'Hair, *Organometallics*, 2012, **31**, 8012.
36 (*a*) G. N. Khairallah, T. Waters and R. A. J. O'Hair, *Dalton Trans.*, 2009, 2832; (*b*) G. N. Khairallah, C. M. Williams, S. Chow and R. A. J. O'Hair, *Dalton Trans.*, 2013, DOI: 10.1039/C2DT32143B, in press.
37 C. Brunet, R. Antoine, M. Broyer, P. Dugourd, A. Kulesza, J. Petersen, M. I. S. Röhr, R. Mitrić, V. Bonačić-Koutecký and R. A. J. O'Hair, *J. Phys. Chem. A*, 2011, **115**, 9120.
38 Fixed-charged ligands have been used to probe the formation and reactions of organometallic reagents: (*a*) D. M. Chisholm and J. S. McIndoe, *Dalton Trans.*, 2008, 3933; (*b*) K. Koszinowski, *J. Am. Chem. Soc.*, 2010, **132**, 6032; (*c*) K. L. Vikse, M. A. Henderson, A. G. Oliver and J. S. McIndoe, *Chem. Commun.*, 2010, **46**, 7412; (*d*) K. L. Vikse, S. Kwok, R. McDonald, A. G. Oliver and J. S. McIndoe, *J. Organomet. Chem.*, 2012, **716**, 252; (*e*) N. J. Farrer, K. L. Vikse, R. McDonald and J. S. McIndoe, *Eur. J. Inorg. Chem.*, 2012, **2012**, 733.
39 For the use of fixed-charge substrates to monitor the formation of products of metal-catalyzed reactions see: (*a*) K. L. Vikse, Z. Ahmadi, C. C. Manning, D. A. Harrington and J. S. McIndoe, *Angew. Chem., Int. Ed.*, 2011, **50**, 8304; (*b*) M. A. Henderson, J. Luo, A. G. Oliver and J. S. McIndoe, *Organometallics*, 2011, **30**, 5471; (*c*) M. A. Schade, J. E. Fleckenstein, P. Knochel and K. Koszinowski, *J. Org. Chem.*, 2010, **75**, 6848, and references cited therein.
40 C. P. G. Butcher, A. Dinca, P. J. Dyson, B. F. G. Johnson, P. R. R. Langridge-Smith and J. S. McIndoe, *Angew. Chem., Int. Ed.*, 2003, **42**, 5752.
41 C. P. G. Butcher, P. J. Dyson, B. F. G. Johnson, J. S. McIndoe, P. R. R. Langridge-Smith and C. Whyte, *Rapid Commun. Mass Spectrom.*, 2002, **16**, 1595.
42 S. L. G. Husheer, O. Forest, M. Henderson and J. S. McIndoe, *Rapid Commun. Mass Spectrom.*, 2005, **19**, 1352.
43 M. R. Barton, Z. Yuegang and J. D. Atwood, *J. Coord. Chem.*, 2002, **55**, 969.
44 (*a*) W. A. Donald, C. J. McKenzie and R. A. J. O'Hair, *Angew. Chem., Int. Ed.*, 2011, **50**, 8379; (*b*) A. K. Y. Lam, C. Li, G. N. Khairallah, B. B. Kirk, S. J. Blanksby, A. J. Trevitt, U. Wille, R. A. J. O'Hair and G. da Silva, *Phys. Chem. Chem. Phys.*, 2012, **14**, 2417.
45 M. J. Frisch, *Gaussian 09 (Revision B.01)*. Gaussian, Inc., Wallingford, CT, 2010. See ESI† for complete citation.
46 A. D. Becke, *J. Chem. Phys.*, 1993, **98**, 5648.
47 C. Lee, W. Yang and R. G. Parr, *Phys. Rev. B: Condens. Matter*, 1988, **37**, 785.
48 M. Dolg, U. Wedig, H. Stoll and H. Preuss, *J. Chem. Phys.*, 1987, **86**, 866.
49 P. C. Hariharan and J. A. Pople, *Theor. Chim. Acta*, 1973, **28**, 213.
50 T. Clark, J. Chandrasekhar and P. V. R. Schleyer, *J. Comput. Chem.*, 1983, **4**, 294.
51 R. Krishnam, J. S. Binkley, R. Seeger and J. A. Pople, *J. Chem. Phys.*, 1980, **72**, 650.
52 P. M. W. Gill, B. G. Johnson, J. A. Pople and M. J. Frisch, *Chem. Phys. Lett.*, 1992, **197**, 499.
53 O. Stelzer, S. Rossenbach and D. Hoff, *Catalysis for an Aqueous Catalysisk: Section 3.2*, Wiley-VCH Verlag GmbH & Co. KGaA, 2005; pp. 100–197.
54 C. A. Tolman, *Chem. Rev.*, 1977, **77**, 313.
55 E. Vergara, E. Cerrada, C. Clavel, A. Casini and M. Laguna, *Dalton Trans.*, 2011, **40**, 10927.
56 B. Biswas, M. Sugimoto and S. Sakaki, *Organometallics*, 2000, **19**, 3895.
57 M.-E. Moret, S. F. Keller, J. C. Slootweg and P. Chen, *Inorg. Chem.*, 2009, **48**, 6972.
58 B. Hammond, F. H. Jardine and A. G. Vohra, *J. Inorg. Nucl. Chem.*, 1971, **33**, 1017.
59 D. J. Darensbourg, M. W. Holtcamp, B. Kahandelwal and J. H. Reibenspies, *Inorg. Chem.*, 1994, **33**, 531.
60 D. J. Darensbourg, M. W. Holtcamp, E. M. Longridge, B. Khandelwal, K. K. Klausmeyer and J. H. Reibenspies, *J. Am. Chem. Soc.*, 1995, **117**, 318.
61 J. Granatier, M. Urban and A. J. Sadlej, *Chem. Phys. Lett.*, 2010, **484**, 154.